Engineering Structures 31 (2009) 1997–2008

Contents lists available at ScienceDirect

Engineering Structures

journal homepage: www.elsevier.com/locate/engstruct

Seismic performance of steel structures with slit dampers

Sang-Hoon Oh [a], Young-Ju Kim [b,*], Hong-Sik Ryu [c]

[a] School of Architecture, Pusan National University, 30 Jangjeon-dong, Geumjeong-gu, Busan 609-735, Republic of Korea

[b] Department of Civil, Environmental and Architectural Engineering, Korea University, 5 Anam-dong, Seongbuk-Gu, Seoul 136-701, Republic of Korea

[c] Research Institute of Industrial Science & Technology (RIST), 79 Youngcheon Dongtan, Hwasung, Kyoungkido, 445–810, Republic of Korea

ARTICLE INFO

Article history:
Received 8 July 2008
Received in revised form
8 December 2008
Accepted 6 March 2009
Available online 5 April 2009

Keywords:
Beam-to-column connection
Slit damper
Repair
Elastic stiffness
Deformation capacity

ABSTRACT

During the Northridge and Kobe Earthquakes, many steel moment resisting frames suffered damage at the beam-to-column connections. In order to solve this problem, an innovative structural system with slit dampers was developed in this study, which could not only provide good seismic performance but could also be easily repaired after a heavy earthquake. In the proposed structural system, a mechanical joint is adopted that is equipped with a metallic damper as the beam-to-column connection. The main feature of this system is that plastic deformation is limited to the slit dampers at the bottom flange. The seismic performance of the proposed connection was verified through cyclic tests of three full-scale steel structures that had slit dampers and of one specimen that had a conventional welded moment resisting frame. Test results indicated that the proposed connection showed an excellent hysteretic behavior. In addition, the energy dissipation and plastic deformation in this system were concentrated only at the slit dampers, while the inelastic behavior of the beams and columns is prevented through appropriate capacity design.

1. Introduction

During the Northridge (1994) and Kobe (1995) earthquakes, while many buildings were designed to avoid collapse, thus saving human lives [1,2], a large number of steel buildings suffered severe damage, where structural functions were destroyed. The most severe damage appeared to be brittle fractures at welded beam-to-column connections. While such damage was inevitable for older steel structures that have nonductile connection details, it was also expected for some relatively new buildings designed in accordance with the current seismic codes [3,4]. Subsequent studies mostly focused on understanding the causes of damage to steel structures, assessing major parameters that affect the cyclic behavior of steel moment connections, and recommending improvements to these connections. After the Northridge and Kobe earthquakes, important experimental programs on beam-to-column connections were developed in the USA and Japan as follows: the reduced beam section (RBS) [5–8], the cover plate or haunch [9,10], no weld access hole [6,11,12], and improved weld access hole [13–15]. Although these improved connections have shown satisfactory performance in the laboratory, the seismic design of these details is based on the plastic rotation capacity of main members within the frame such as the beam and column. Thereby, when these details are used, damaged buildings cannot be easily repaired. Since it is important to restore buildings and the functions of the effected urban area as quickly as possible after an earthquake, these welded connection details are not effective when attempting to solve the issues caused by recent disasters.

To overcome these types of problems, a damage-controlled structure has previously been proposed that uses passive energy dissipation devices [16]. Passive energy dissipation systems have been considered as an effective and inexpensive way to mitigate earthquake risks to structures. Since the Northridge earthquake, passive damping technologies have been increasingly taken into consideration in the USA, and since the Kobe earthquake in Japan, more buildings have been designed to include dampers [17,18]. The main reason for using passive energy dissipation devices in a structure is to limit the number of damaging deformations in structural components. Among the available varieties of passive energy dissipation devices, the metallic-hysteretic damper is one of the most effective and economical mechanisms for the dissipation of seismic energy input, which is obtained through the inelastic deformation of metallic material. Numerous metallic dampers have been proposed: TADAS [19], the honeycomb damper [20], the buckling-restrained brace (BRB) [21–24], and the slit damper [25–28]. These devices are mainly designed to be incorporated into the bracing system of structural frames. Other devices have been developed to be installed between beams and columns in a frame structure [29–32].

This present study proposes a new steel structure that achieves structural performance and is easily repairable after an earthquake.

* Corresponding author. Tel.: +82 2 9217 983; fax: +82 2 921 2439.
E-mail address: kyj282@empal.com (Y.-J. Kim).

0141-0296/$ – see front matter © 2009 Elsevier Ltd. All rights reserved.
doi:10.1016/j.engstruct.2009.03.003

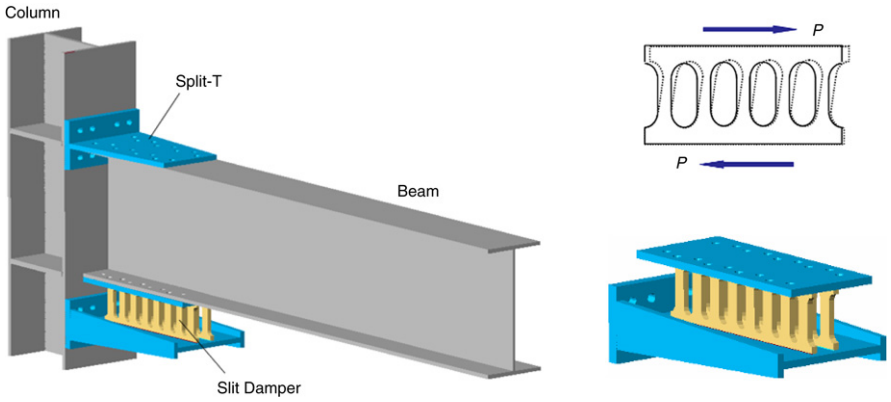

Fig. 1. The proposed beam-to-column connection detail with slit damper.

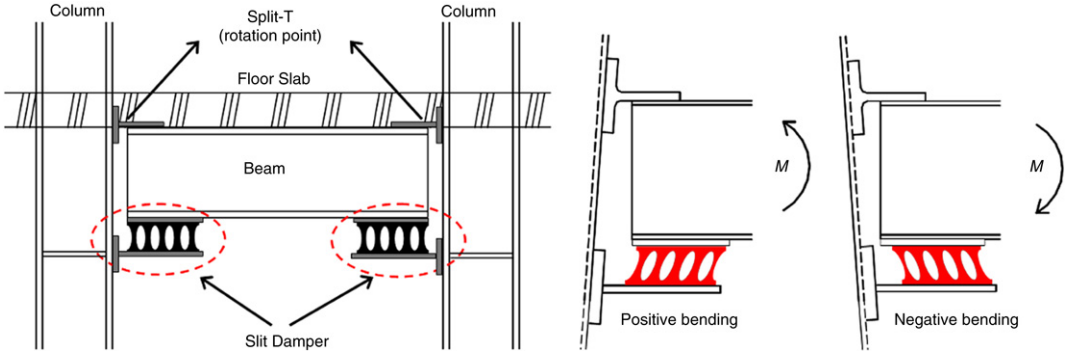

Fig. 2. The proposed connection system and deformation.

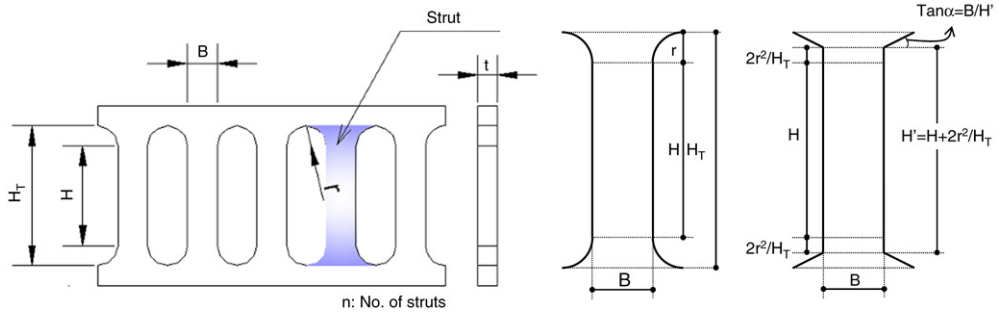

Fig. 3. Idealization of slit damper.

The main feature of this system is that plastic deformation is limited to the slit dampers at the bottom flange of the beam-ends. The structural configuration and mechanical characteristics of the proposed structural system are addressed in this paper. In the proposed structural system, the mechanical joint was adopted that was equipped with a metallic damper as the beam-to-column connection. Cyclic tests were conducted quasi-statically on three full-scale subassemblages that had slit dampers and on one specimen that had a conventional post-Northridge welded connection. The mechanical behavior of the entire connection system was also evaluated theoretically and mathematical models were formulated to provide stiffness and strength predictions.

2. New beam-to-column connection systems

2.1. Structural configuration

To determine the optimum damage control design of the frame, it is desirable to construct structures that can be easily repairable, and to facilitate replacement after the earthquake by limiting the damage to the energy absorption devices. Accordingly, if the dampers on which the damage is concentrated are connected to a main frame by exchangeable high-strength bolts, the beams and columns are easier to repair than with welded connections. By designing dampers that are weaker than the beam and column, it is possible to limit damage to the dampers. The split-T connection is a typical example of the use of high-strength bolts on existing beam-to-column connections. While the advantages of this connection are the simple construction and superior stiffness of the connection, the compression force can cause local buckling on the beam flange. During an earthquake, it is preferable that the damage be limited to those energy absorption elements that have good hysteretic characteristics and not be transmitted to the main frame such as the beam and column.

Fig. 1 shows the new connection system with the energy absorption element proposed in this study. The slit damper on the bottom flange of the beam is actively plasticized before the main structural members. This system takes post-earthquake repairs

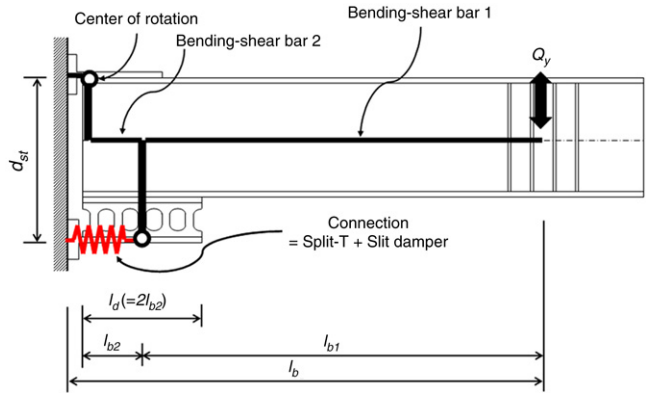

Fig. 4. Analytical model of proposed connection.

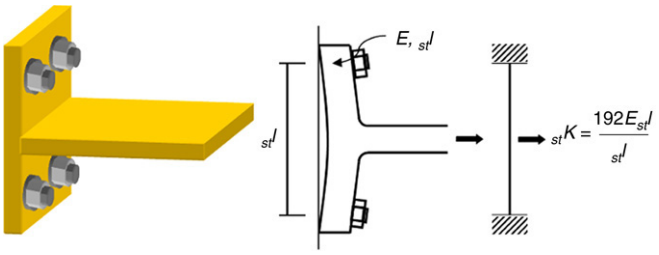

Fig. 5. Deformation of split-T.

into consideration as well as the presence of concrete slabs. High-strength bolts are used to connect all columns and beams. That is, the upper split-T is connected with high-strength bolts at the top of the beam to serve as the rotational center of the connection, while the lower split-T is connected with high-strength bolts to concentrate the deformation to the slit dampers of the bottom flange. As shown in Fig. 2, since the rotation points on the left and right sides stay at the top flange, damage to the split-T on the top flange, which is difficult to exchange, is avoided. It is expected that deformation of a structure is concentrated on the slit dampers at the bottom flange, if the slit dampers show the same behaviors in positive bending (when the top flange is under compression) and negative bending (when the top flange is under tension). As a result, the dampers can freely deform at the bottom flange of the beam without causing significant damage to the concrete slab under large story drifts. This design permits the simple replacement of slit dampers as connection elements of the bottom flange, allowing the continued use of buildings after an earthquake. Since the major retrofit work after an earthquake is performed near the bottom flange, the slabs do not need to be removed. Furthermore, it is not necessary to consider the influence of the resulting uplift of the neutral axis position due to the constraint effect of the floor slabs.

The proposed structural system employs the connection between the beam top flange and the column flange as a means of transferring gravity loads from the beams to the columns. Also, the split-T at the top flange can be kept in an elastic range because the center of rotation stays at the top flange of the beam. Thus, using this system, when the structure suffers compulsory deformation under an earthquake, the deformation is concentrated on the dampers at the bottom flange. Because the plastic deformation of the proposed structural system is concentrated on the dampers in the beam-ends, this system can be regarded as a "strong column-weak beam" when considering the plastic hinge of beam-ends.

2.2. Slit damper design

To ensure that the proposed beam-to-column connection system operates correctly, it is necessary to have a stable and large energy dissipative capacity at the bottom flange, which can be deformed evenly under repeated loads, i.e. under the tensile and compressive force on the bottom flange. To limit damage to the connection element without causing damage to the main structural members, it is necessary for the connection to have relatively high stiffness that yields ahead of the key structural members. The energy is dissipated through plastic deformation on the vertical struts of the slit dampers, as shown in Fig. 1. It has been previously reported that the slit damper has an extremely good energy dissipative capacity as well as high stiffness and is considered appropriate to use as a connection element in the system proposed in this study [25,26].

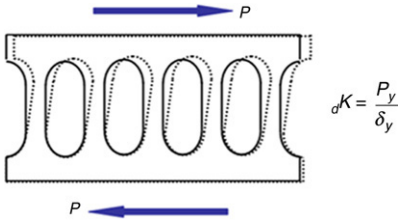

Fig. 6. Deformation of slit damper.

For the purpose of predicting the yield strength and deformation of the slit damper, the struts of the damper were idealized as shown in Fig. 3, where the round-shaped ends have been replaced with straight lines [25]. By using this simplification, the yielding strength and apparent maximum strength of the slit damper can be obtained analytically as follows:

$$P_y = \min\left\{n\frac{\sigma_y tB^2}{2H'}, n\frac{2\sigma_y tB}{3\sqrt{3}}\right\} \quad (1)$$

$$P_u = \min\left\{n\frac{\sigma_u tB^2}{2H'}, n\frac{2\sigma_u tB}{3\sqrt{3}}\right\}. \quad (2)$$

In Eqs. (1) and (2), the first term means that the yielding of the slit damper is governed by the flexural moment, while the second term means that the yielding of the slit damper is governed by shear force. Where n = the number of struts on the slit damper; t = the thickness of the plate; σ_y = the yield stress; σ_u = the maximum stress; B = the width of the struts and H' = the equivalent height indicated in Fig. 3 ($H' = H + 2r^2/H_T$). The factor 2/3 in the second term of Eqs. (1) and (2) accounts for the fact that, within the elastic range, when the aspect ratio of the plate B/H is less than 1.0, the relationship between the average shear stress and the maximum shear stress is 2/3. The yield displacement of the slit damper can be analytically expressed and simplified by the following elastic-based equation [25,26].

$$\delta_y = \frac{1.5P_yH_T}{nEtB}\left[\left(\frac{H'}{B}\right)^2 + 2.6\right]. \quad (3)$$

Here E is the Young's modulus and H_T is the total height of the strut of the slit damper.

2.3. Lateral load-carrying capacity

2.3.1. Evaluation of initial stiffness

As shown in Fig. 4, the lateral stiffness of the connection made by using the slit damper was derived from a simple connection model. The beams were modeled into the bending-shear bar 1, where the distance from the loading point to the center of the slit damper is considered to be the effective length (l_{b1}), and into the bending-shear bar 2, where the distance from the center of the damper to the beam-end is considered to be the effective length (l_{b2}). The upper split-T was modeled as a pin, as the rotational

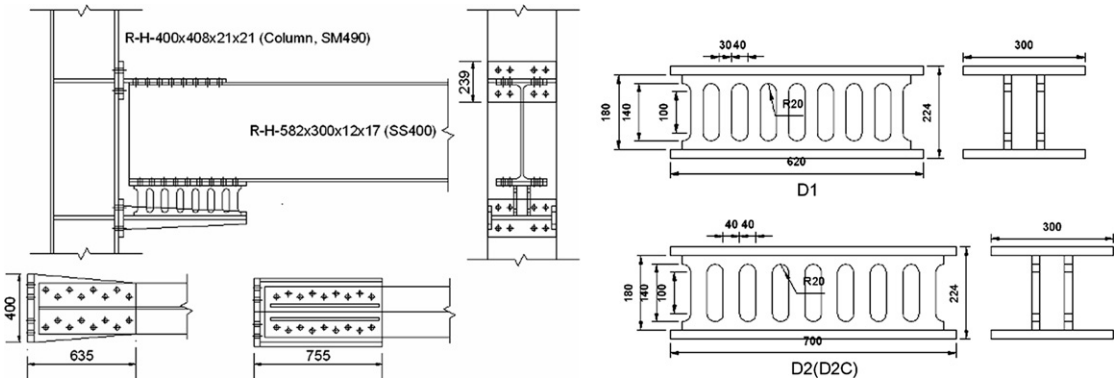

(a) D1 and D2 (D2C).

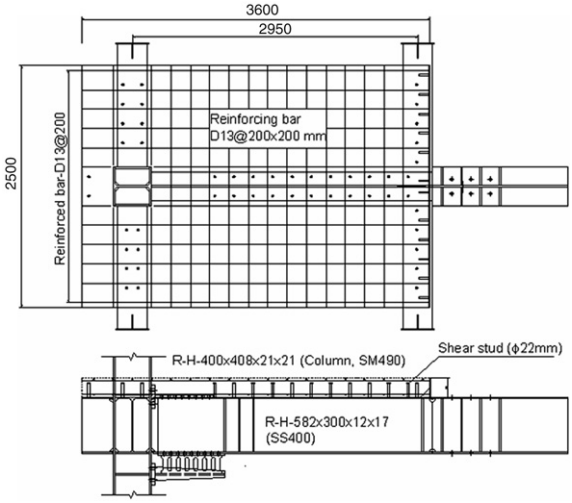

(b) Composite specimen (D2C).

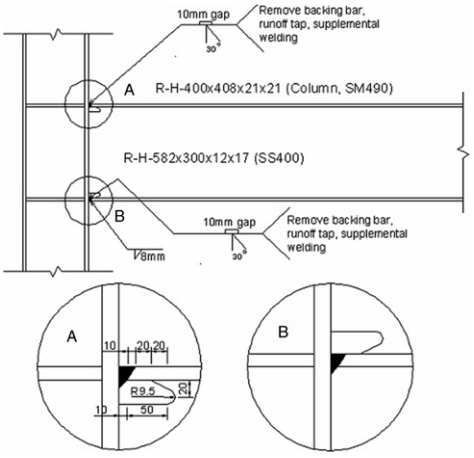

(c) welded specimen (W).

Fig. 7. Details of specimens.

center of the connection. The flexural stiffness of the column was considered to be significantly stiff for the sake of the simplification of the model. The connection consisted of a split-T and slit damper and was a representation of the out-of-plane flexural stiffness of the flange of the split-T and the bending or shear stiffness of the slit damper as the serial spring in Fig. 4. The flange of the lower split-T was modeled so that the load was concentrated at the center of the beam, which is fixed at both ends (Fig. 5), and the initial stiffness of the slit damper was obtained based on Eqs. (1) and (3), as shown in Fig. 6.

The initial stiffness of a proposed connection K, defined as the beam shear force divided by the beam tip displacement, can be expressed by:

$$K^{-1} = {}_{b1}K^{-1} + {}_{b2}K^{-1} + {}_{\mathrm{con}}K^{-1}, \tag{4}$$

where ${}_{b1}K^{-1}$, ${}_{b2}K^{-1}$, and ${}_{\mathrm{con}}K^{-1}$ = the initial stiffness that relates the beam shear force to a component of the beam tip displacement caused by deformations of the bending-shear beam 1, bending-shear beam 2, and connection composed by the lower split-T and slit damper, respectively. Applying the principle of virtual forces, each term in Eq. (4) can be obtained as follows:

$${}_{b1}K^{-1} = \frac{l_{b1}^3}{3E_{b1}I} + \frac{l_{b1}}{{}_wAG} \tag{5}$$

$${}_{b2}K^{-1} = \frac{l_{b2}(l_{b1}^2 + l_{b1}l_{b2} + l_{b2}^2)}{3E_{b2}I} + \frac{2l_{b2}}{{}_wAG} \tag{6}$$

$$\begin{aligned} {}_{\mathrm{con}}K^{-1} &= {}_{\mathrm{con}}k^{-1}\left(\frac{l_b}{d_{st}}\right)^2 \\ {}_{\mathrm{con}}k^{-1} &= {}_{st}K^{-1} + {}_dK^{-1} \\ {}_{st}K &= \frac{192E_{st}I}{{}_{st}l}, \qquad {}_dK = \frac{P_y}{\delta_y}. \end{aligned} \tag{7}$$

The stiffness of the bending-shear bar 1 was calculated by using the moment of inertia (${}_{b1}I$) where the gross section of the beam is effective, but only the section of the beam web is effective in the case of shear. The stiffness of bending-shear bar 2 was calculated by using the moment of inertia (${}_{b2}I$), which is effective only on the top flange of the beam, and the shear, which is effective only for a half section of the beam web (${}_wA/2$). Here, l_{b1} and l_{b2} = the length of bending-shear bar 1 and bending-shear bar 2, respectively; ${}_wA$ = the cross-sectional area of the beam web; ${}_{st}l$ = the width of the split-T flange; d_{st} = the distance between the upper split-T and the lower split-T; ${}_{st}K$ and ${}_dK$ = the lateral stiffness of the split-T flange and slit damper, respectively; P_y and δ_y = the yield strength and the displacement of the damper, respectively; and E and G = Young's and shear moduli, respectively.

2.3.2. Yield and maximum strength

Presuming that plastic deformation in the proposed structural system is limited to the slit damper at the bottom flange, this system is capable of carrying the moment from the beam through a couple of forces exerted on the lower split-T connected with the slit damper and on the upper split-T. This moment-carrying

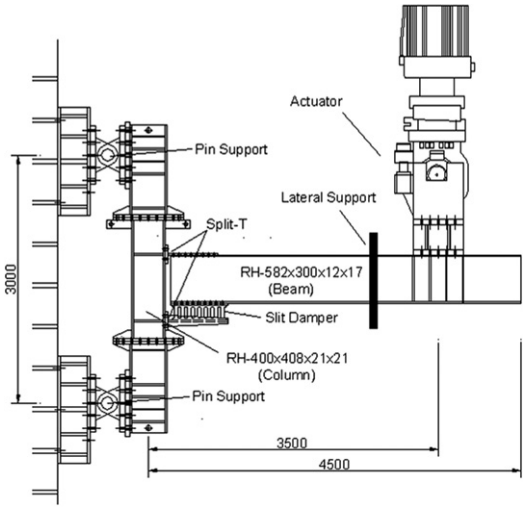

Fig. 8. Test setup.

mechanism beneficially reduces the bending moment in the beam and in the lower column, compared to the moment distribution in the welded moment connection. At the full plastic state, defined at the yielding of the slit damper, the theoretical beam shear force (Q_y) and the moment at the column face (M_y) are expressed by:

$$Q_y = \frac{P_y d_{st}}{l_{b1}} \tag{8}$$

$$M_y = Q_y \cdot l_b = \frac{P_y d_{st} l_b}{l_{b1}}. \tag{9}$$

At the ultimate state, the maximum beam shear force (Q_u) and the moment at the column face (M_u) corresponding to the maximum strength of the slit damper are computed by:

$$Q_u = \frac{P_u d_{st}}{l_{b1}} \tag{10}$$

$$M_u = Q_u \cdot l_b = \frac{P_u d_{st} l_b}{l_{b1}}. \tag{11}$$

3. Test program

3.1. Test specimens

Large-scale structural testing was performed to investigate a comparison of the cyclic performance between the proposed steel structures that have slit dampers and that of a conventional welded moment resisting frame. A total of four specimens of beam-to-column connections were fabricated. Two pure steel specimens with slit damper are designated as D1 and D2, and one composite specimen with a slit damper is designated as D2C. The difference between specimen D1 and D2 is the detail of the slit damper, which was designed to achieve different ratios of the beam's moment demand to its flexural strength. The difference between the D2 and D2C specimens where the same slit dampers were used is the presence of the floor slab. A conventional welded beam-to-column connection, designated as W, was constructed in order to provide a comparison for the proposed connections that have a slit damper.

The test specimen is an external T-shaped model composed of a wide flange beam and column. The beam was an H-582x302x12x17 and the column was an H-400x400x21x21. In terms of the proposed connection between the beam and column, a split-T connection element was used on the top of the beam, and the energy absorption elements constructed by welding the steel slit plate to the split-T was used at the bottom of the beam. High-strength bolts were used to facilitate installation and removal. The frictional connection and the tensile connection of the test specimens constructed with high-strength bolts (F10T) had sufficient connection strength so that the connection would not separate or slip until the slit plate of each test specimen demonstrated maximum strength. Steel grades KS SS400 and SM490 were selected for the beams and columns, respectively. For the slit dampers, the slit plate was manufactured of mild steel KS SS400. The mechanical properties of these steel materials are summarized in Table 1.

Table 2 and Fig. 7 show the list and details of four full-scale specimens, of which there were three that had slit dampers attached. As mentioned previously, the main feature of this proposed system is that plastic deformation is limited to the slit dampers at the bottom flange of the beam-ends. Therefore, the beams of specimens D1 and D2 were designed to remain in the elastic range until the ultimate state. This means that the maximum bending moment in the beam ($_bM_m$) developed by the slit dampers is limited below the beam plastic moment ($_bM_p$). The ratio of maximum bending moment to the beam plastic moment is 0.34 and 0.63 for specimens D1 and D2, respectively. The maximum bending moment in the beam at the end of the slit damper was computed with the magnitude of $Q_u(l_{b1} - l_d/2)$. Referring to previous experimental results [25,28], the peak strength of the slit damper was larger than its respective yield strength (computed by using the yield stress of material) and maximum strength (computed by using the tensile stress of material) by a factor of about 2.0 and 1.3, respectively, which is due to the strain hardening effect of steel materials.

To identify the constraint effect of the floor slab from the proposed system, the connection with the composite beam was designed as shown in Fig. 7(b). To simulate an actual steel building, four side beams were designed at each column web and at each side of loading, and were bonded to the slab using 22 mm diameter shear studs, which were designed to be approximately 80% composite. The 200 mm thick by 2500 mm wide concrete slab was constructed of common concrete having a design strength of 24 MPa. Also, the concrete slab was provided with longitudinal and transverse steel reinforcement. For reinforcement, D13 (13 mm diameter steel reinforcing) bars having a design strength of 400 MPa were placed transversely at 200 mm intervals through the entire length of the concrete slab and were located at 30 mm from both the top and from the bottom of the slab. In addition, a mould plate for slip prevention was installed between the beam flange and the concrete slab, as shown in Fig. 7(b). The presence of the concrete slabs had an effect on the neutral axis location and the plastic zone of the connection. These influences caused a significantly larger strain on the bottom flange than that on the top flange, thereby giving rise to a brittle fracture at the bottom flange. Consequently, the deformation capacity of a composite connection was nearly half that of a steel beam connection [33,34]. However, since the plastic deformation of the proposed structural system is concentrated on the dampers in the bottom flange, it is thought that the influence of the constraint effect of the floor slabs decreases. The test results for specimen D2C are discussed with emphases on the initial stiffness, the ultimate strength, and the beam's strain profiles.

Test specimen W is a welded moment connection that has a weld access hole similar to that of the post-Northridge details. It was designed according to the recommendation of FEMA-350 [8]. Supplemental welding was also carried out after removing the backing bar at the top and bottom flanges of the beam, as shown in Fig. 7(c). Jones et al. [35] indicated that the use of a welded web connection does provide some benefit to the connection performance as it tends to reduce the vulnerability of the weld

Table 1
Mechanical properties of steel materials.

Test specimen		Steel grade	σ_y (MPa)	σ_u (MPa)	Y.R (%)	Elo. (%)
Beam	Web ($t = 12$ mm)	SS400	339	488	70	27
	Flange ($t = 17$ mm)	SS400	318	480	67	30
Column	Web ($t = 20$ mm)	SM490	395	554	74	27
	Flange ($t = 20$ mm)	SM490	378	551	71	24
Split-T	Web ($t = 22$ mm)	SM490	388	577	71	25
	Flange ($t = 35$ mm)	SM490	386	573	69	24
Slit plate ($t = 19$ mm)		SS400	208	464	63	30

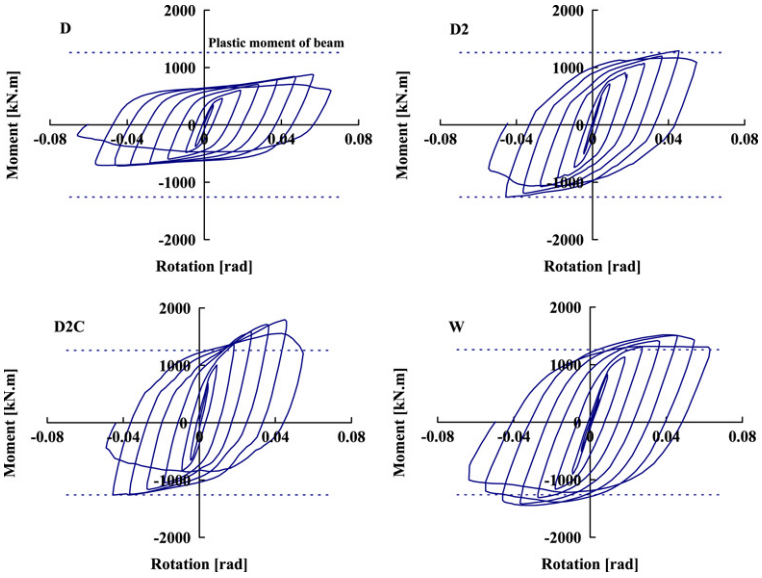

Fig. 9. Moment versus rotation relationship.

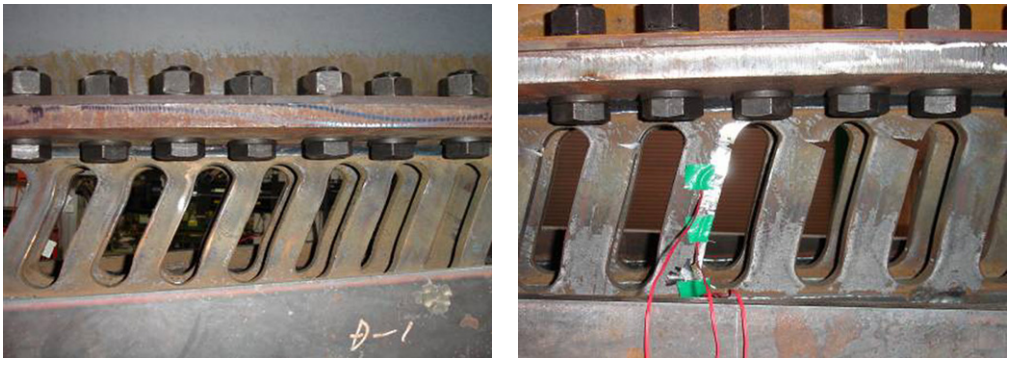

(a) Damper deformation of specimen D1.

(b) Damper failure of specimen D2.

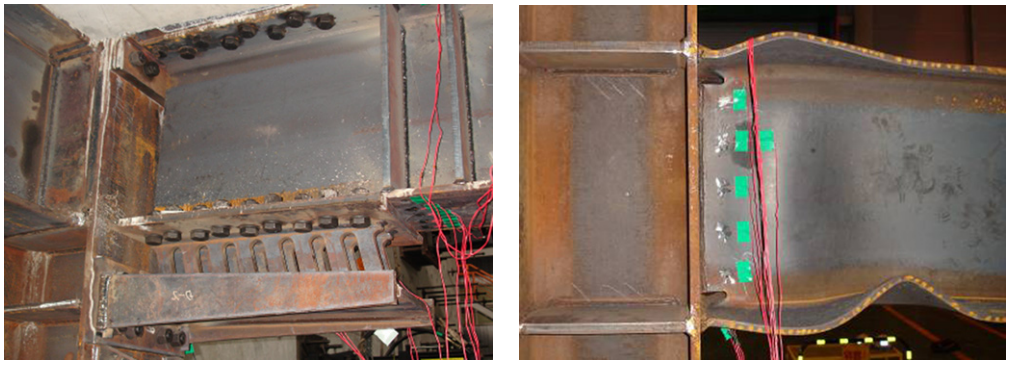

(c) Damper deformation of specimen D2C.

(d) Beam local buckling of specimen *W*.

Fig. 10. Photograph of specimens after testing.

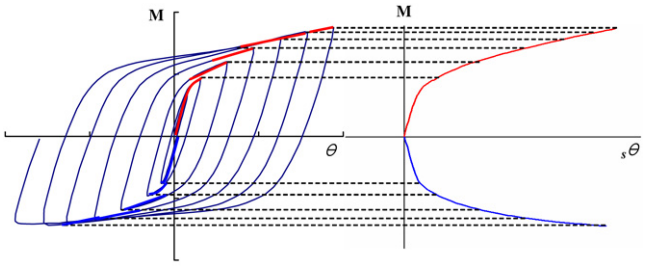

Fig. 11. Concept of skeleton curve.

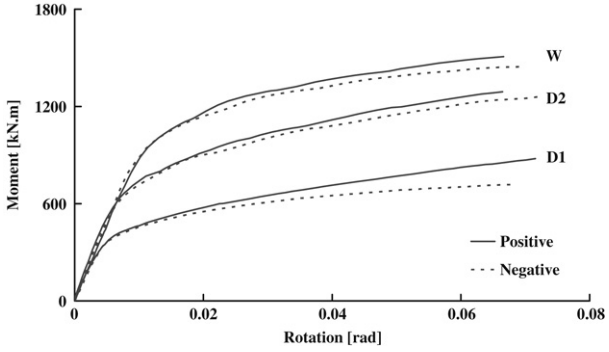

Fig. 12. Skeleton curves of steel specimens.

fracture. Therefore, specimen *W* was designed using a fully welded beam web. This connection specimen was constructed as a baseline specimen in order to provide a comparison with the proposed damper connection in terms of the initial stiffness, hysteretic characteristics, and the collapse mode.

3.2. Loading device and loading method

The test setup was designed to simulate the boundary conditions of a beam-to-column connection subassembly in a moment resisting frame under typical lateral loading. The test setup was thus created by using pins to support both ends of the vertical column, and by connecting the actuator to the loading point of the beam, as shown in Fig. 8. The distance between the column center and the loading point was 3500 mm, and the column was supported with pins on both points. The distance between points was 3000 mm. To prevent an out-of-plane deformation of the beam during loading, lateral supports were installed on the beam. The loading protocol prescribed a quasi-static cyclic pattern defined in terms of a connection rotation. After applying the elastic loading of $\pm 1\theta_y$, based on the displacement of the loading point, an incremental displacement control was applied, based on $\pm 2\theta_y$, $\pm 4\theta_y$, $\pm 6\theta_y$, etc. Here, the term, θ_y, is the yield rotation corresponding to the plastic moment of the steel beam. The direction of the loading and the displacement were regarded as "positive" when loading was applied upward. In addition, the specimen was equipped with displacement transducers and strain gauges to measure the deformation contributions of different parts and the strain distributions, respectively.

4. Test results and discussion

4.1. Hysterectic behavior

Fig. 9 shows the moment versus rotation relationship of each specimen. The dashed line in Fig. 9 represents the fully plastic moment of the beam (1260 kN m) calculated by using the material

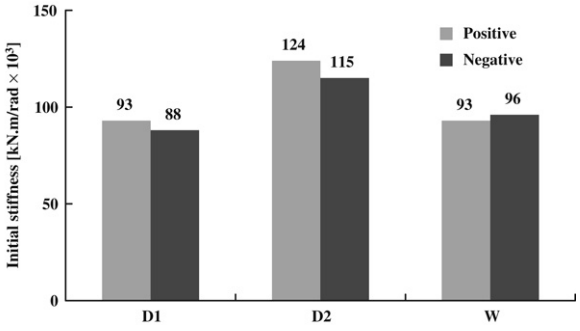

Fig. 13. Initial stiffness.

Table 2
List of test specimens.

Specimen	Slit damper					Floor slab
	B (mm)	*t* (mm)	*H* (mm)	*r* (mm)	*n* (EA)	
D1	30	19	100	20	16	None
D2	40	19	100	20	16	None
D2C	40	19	100	20	16	Yes
W	Welded moment connection					None

Table 3
Comparison between experimental result and analytical result.

Specimen	Initial stiffness kN m/rad			Yield moment kN m		
	${}_pK$	${}_eK_P$	${}_eK_N$	${}_pM_y$	${}_eM_{yP}$	${}_eM_{yN}$
D1	107 000	93 000	88 000	351	385	372
D2	147 000	124 000	115 000	632	672	653

properties in Table 1. Fig. 10 shows a photograph of the specimens after testing.

As observed in Fig. 9, the proposed specimens exhibited stable hysteretic behavior until the ultimate state was reached during 0.04 rad story drift cycles. During loading, D1, D2, and D2C sustained plastic deformation only at the slit dampers without any signs of damage to other parts of the structures, as shown in Fig. 10(a)–(c). The plots also showed that the slit dampers were capable of sustaining a large number of cycles under significant plastic deformations. Strength degradation started to appear when cracks slowly formed at the ends of the struts due to stress concentration. On average this took place shortly after 0.04 rad story drift cycles of loading. The tests were stopped after almost all the struts in the dampers were completely fractured and when the sustained load was significantly reduced. The maximum strength of specimen D1 did not arrive at the beam plastic moment, while the maximum strength of specimen D2 was almost the same as the beam plastic moment, even though the ratio of the maximum strength to the beam plastic moment is equal to 0.63. This result indicates that the hysteretic behavior of slit dampers is essentially governed by the strain hardening under load reversals.

Test specimen D2C was constructed by adding a floor slab to test specimen D2. Due to the rise in the neutral axis resulting from the composite effects of the slab, the maximum strength increased in the positive direction by approximately 40% over than that of the steel specimen D2. However, the negative direction showed virtually identical strengths, whereby, despite the presence of slabs, an almost equal strength and deformation capacity were observed in specimen D2. In terms of the failure after test, it was confirmed that deformation was concentrated on the slit damper.

Similarly to the proposed specimens, the conventional welded specimen *W* also exhibited stable hysteretic behavior until the ultimate state was reached. Nevertheless, the test results for specimen *W* showed serious local buckling on the beam, resulting in the creation of a plastic hinge. However, even micro cracks

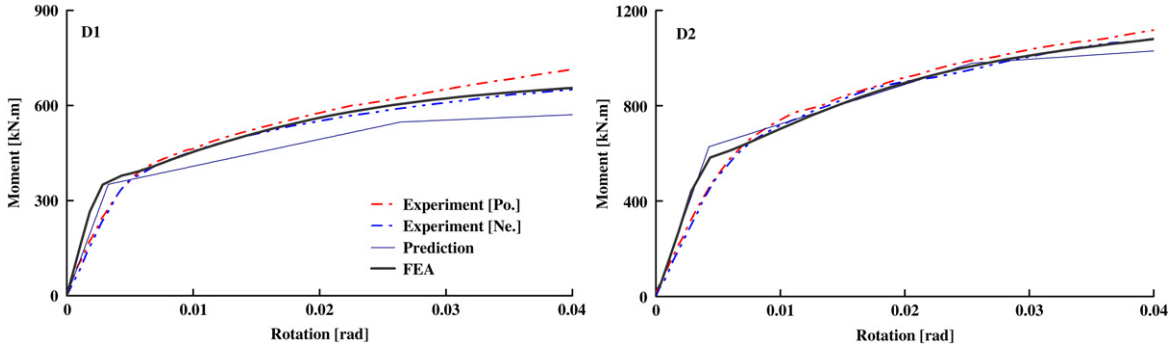

Fig. 14. Comparison of experiment, theory, and FEA in skeleton curve.

were not observed in the area surrounding the improved scallop (Fig. 10 (d)). As expected, the panel zone almost remained within the elastic range due to the strong panel zone. It is believed that the details presented by FEMA 350 show an appropriate connection method that allows for ductile behavior. Nevertheless, the local buckling of the beam as a main structural member does not facilitate repair of the connection. Conversely, the damper connection is considered to be extremely effective in terms of economy, and allows repair work to be performed easily by simply replacing dampers.

Fig. 9 indicates that the plastic rotation of all connections exceeds 0.03 rad. The connection demonstrated an average plastic rotation performance of 0.037 rad. The plastic rotation exceeded 0.03 rad even for the D2C test specimen with a floor slab. This indicates that the superior deformation capacity of the proposed structural system can be demonstrated even when the slab effects are considered.

4.2. Initial stiffness

Skeleton curves are commonly adopted when characterizing the hysteretic behavior and the ductility capacity of steel members that are subjected to load reversals. The concept of a skeleton curve is shown in Fig. 11. A skeleton curve is constructed by connecting skeleton portions; a skeleton portion is defined as part of a restoring force versus deformation curve that exceeds the maximum restoring force achieved in previous loading cycles.

Figs. 12 and 13 show skeleton curves of steel specimens and the bar chart of the initial stiffness, respectively, for comparison of the initial stiffness of each specimen. It was observed that the initial stiffness of specimen D1 was almost equal to that of specimen *W*, while the initial stiffness of test specimen D2 was approximately 30% higher than that of specimen *W*. This result shows that for the proposed system, initial stiffness is governed by the design of the slit damper. Usually, as the strength of the slit damper increases, the initial stiffness also increases. The elastic stiffness and the strength of the slit damper can be adjusted by altering the method of design. For this reason, the results mentioned above show that the proposed connection is more beneficial than the welded connection in controlling the inter-story drift and damage, in the case of the steel moment frame where the energy absorption elements presented in this study were mounted. No problems are indicated with the connection proposed in this study in realizing the moment connection in respect to stiffness.

Table 3 shows a comparison between the experiment and the prediction in terms of initial stiffness of each connection, based on Eqs. (4)–(7). This table indicates that the predicted data is slightly higher than the experimental data. However, the comparison demonstrates that the theoretical formulas support the accuracy and consistency of the experimental findings. Here, ${}_pK$ = the predicted initial stiffness; and ${}_eK_P$ and ${}_eK_N$ = the experimental initial stiffness in positive bending and in negative bending, respectively.

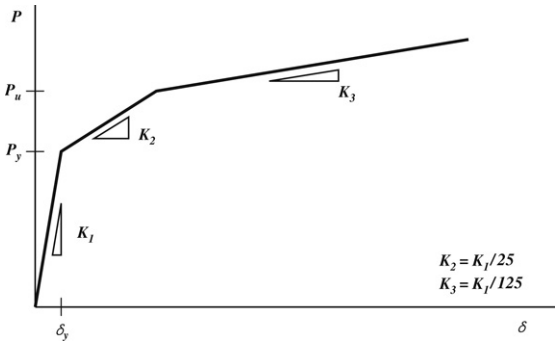

Fig. 15. Idealized trilinear skeleton curve of slit damper.

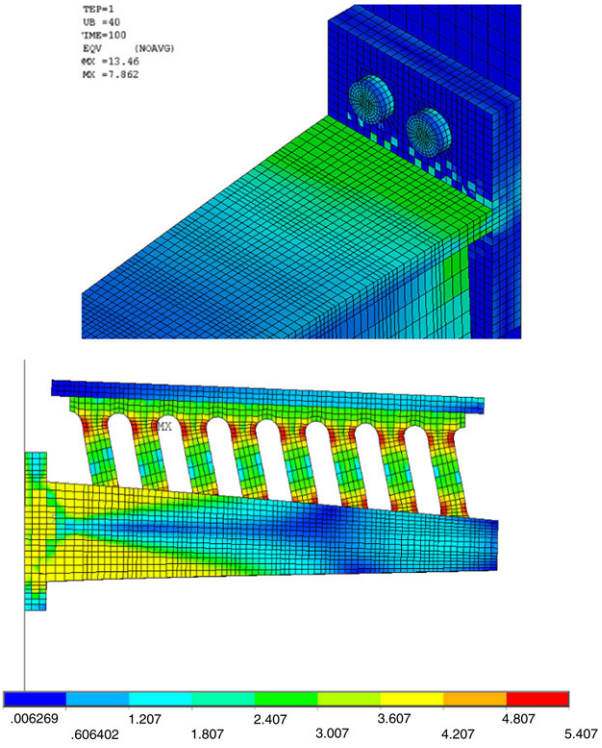

Fig. 16. Von Mises stress contour (Specimen D2).

4.3. Prediction of moment versus rotation curve

The skeleton curves were predicted based on the theoretical formulas provided in 2.3. For comparison, the theoretical initial stiffness and the yield and maximum strength were derived from Eqs. (4), (9) and (11) for the proposed specimens. In Fig. 14, the predicted skeleton curves that were explained in Section 2.3

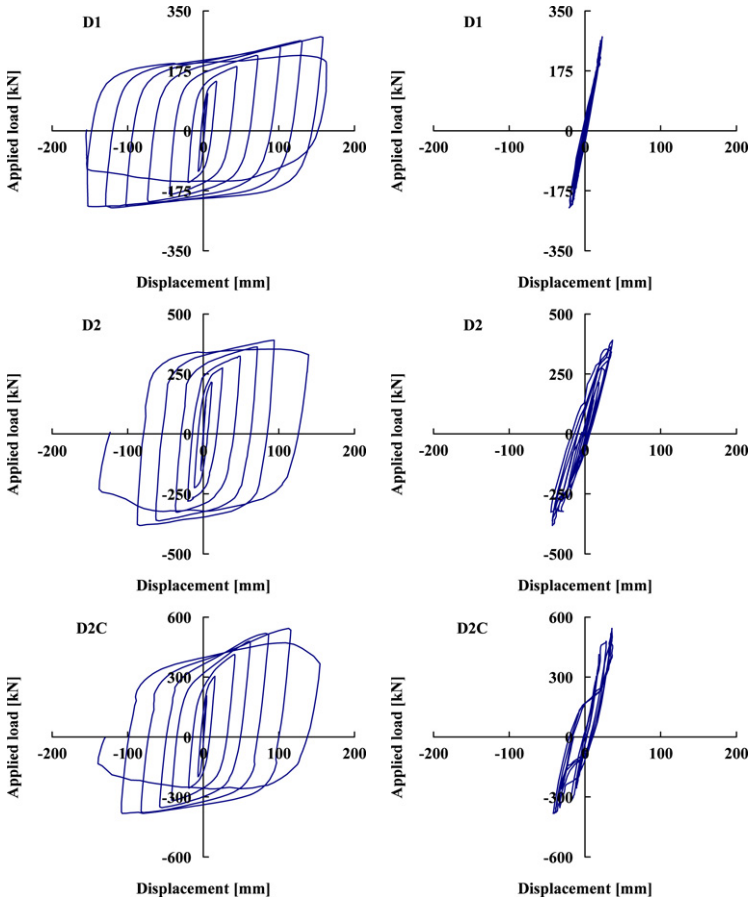

(a) Beam. (b) Damper.

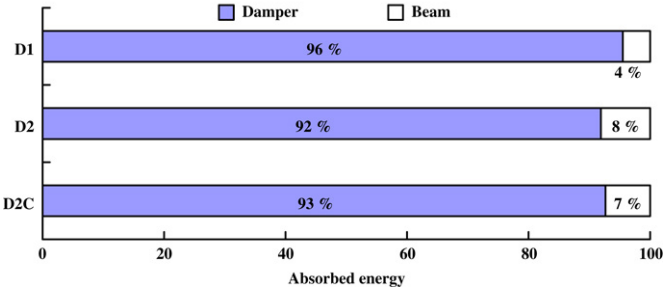

(c) Absorbed energy.

Fig. 17. Hysteresis loops of damper and beam, and contributions of absorbed energy.

were compared with those obtained from the experimental data. Furthermore, the predicted skeleton curve for the slit damper was that obtained from previous research [25], which was idealized with trilinear models, as shown in Fig. 15.

For the proposed specimens, the predicted initial slope of the moment-rotation relationship virtually aligns with the experimental curve as well as the curves obtained by finite element analysis (FEA). The accuracy of the predicted connection strength is also significant. Referring to Table 3, the discrepancy between the predicted and test results of yield strength is approximately ±10%, where ${}_pM_y$ = the predicted yield moment; and ${}_eM_{yP}$ and ${}_eM_{yN}$ = the experimental yield moment in positive bending and in negative bending, respectively. This result indicates that from the comparison of moment versus rotation relationship, the theoretical model adequately describes the behavior of the specimen. In addition, the results obtained from FEA for the proposed structural system were also compared. A nonlinear FEA was carried out [36], in which the proposed connection was represented by solid elements for slit dampers and bolts and by shell elements for beams and columns, the results of which were compared with the skeleton curve from the experiment, as shown in Fig. 14. The elastic and plastic properties of the material were directly obtained from the coupon test. Fig. 16 shows the von Mises stress contour for specimen D2. As can be seen from Fig. 14, the FEA model provided a very accurate prediction of the elasto-plastic response.

4.4. Plastic deformation and energy

For damage-controlled structures, much of the input energy of the earthquake is absorbed by the specific members. The damage is therefore limited to certain members. Fig. 17 plots the shear force versus displacement relationships of the damper and beam for the proposed specimens. Here, 'displacement' denotes the

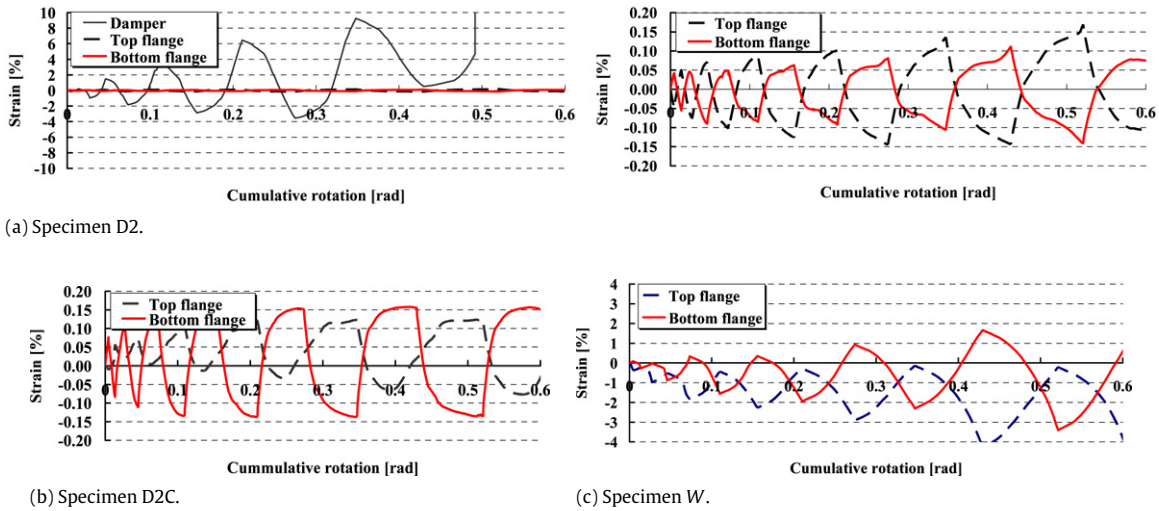

(a) Specimen D2.

(b) Specimen D2C.

(c) Specimen *W*.

Fig. 18. Strain profiles at beam flange and damper.

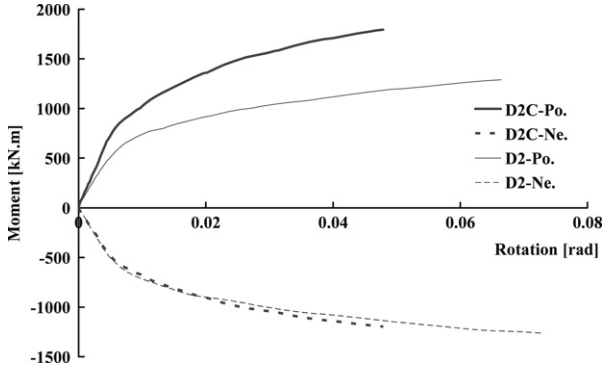

Fig. 19. Comparison of specimens D2 and D2C in skeleton curves.

deformation of the slit damper portion or the beam portion at the loading point. The column and the panel zone of this test specimen were designed to be relatively strong and the elasticity was confirmed through the experiment. For this reason, Fig. 17 represents the curves for only a beam and a damper. Unlike the almost elasto-plastic behavior of the slit dampers, the behavior of the beams was characterized by almost elastic or extremely narrow hysteretic loops (Fig. 17(a) and (b)). From this result, it is worth noting that, in contrast to conventional welded moment connections, the plastic deformation in the proposed structural systems were concentrated only at the slit dampers rather than at the beams.

The damage to the test specimens can be evaluated by means of plastic deformation sustained by the beams. Fig. 17(b) cleary demonstrates the essentially elastic response of specimen D1. The beam of specimens D2 and D2C experienced some yielding as a result of substantial strain hardening engaged in the slit dampers. However, such plastic deformation is apparently insignificant. This observation suggests that it is important to use those beams and slit dampers where the ratio of maximum bending moment to the beam plastic moment is equal to approximately 0.6. Accordingly, plastic deformations will be concentrated only in the slit dampers while the beams and columns almost respond in the elastic range until the ultimate state is reached.

Fig. 17(c) shows the energy shares of each test specimen. The energy of each test specimen was obtained through the area of the hysterectic loop. The energy absorbed by the slit damper constituted approximately an average of 94 % of all absorbed energy. This result indicates that the energy absorption is concentrated primarily at the slit dampers rather than the beams. These slit dampers can be more readily replaced after an earthquake than beam and column structures.

4.5. Strain behavior

Fig. 18 shows the strain profiles of the beam flanges and the slit dampers of the test specimen. The lateral axis shows the cumulative rotation, and the longitudinal axis shows the strain value. In terms of test specimen D2, the maximum strain value in the dampers was approximately 9% and 4% in positive and negative bending, respectively, while the maximum strain value in the beam flange was approximately 0.15% (Fig. 18(a)), which is the elastic response of the beam flange. This result was confirmed through strain profiles, which showed that the beam flange remained in the elastic range until the slit damper reached its ultimate fracture state. Similarly, Fig. 18(b) shows that the strain profiles in the beam flange of specimen D2C, as the composite beam specimen, remain in the elastic range. However, in the case of specimen *W*, the strain of the beam flange was extremely large due to the plastic deformation of the beam as a main member in the structure. The strain profiles reveal that the slit dampers share almost all plastic deformation and the beam members respond almost within the elastic range. Although the welded specimen *W* demonstrated a sound seismic performance by pushing the plastic hinging in the beam, it is ineffective to repair these conventional welded connections after an earthquake.

4.6. Composite effect of floor slab

To investigate the composite beam effect on the ductility of the proposed connections, the skeleton curves for specimens D2 and D2C were compared. Fig. 19 shows the skeleton curves for positive and negative bending in specimens D2 and D2C. Fig. 20 shows the bar charts for the initial stiffness and the maximum moment. The initial stiffness and maximum moment of the connection D2C increased by approximately 1.2 times and 1.4 times that of D2 in positive bending due to the slab effects, respectively. Conversely, the initial stiffness and maximum moment in negative bending were almost identical. The neutral axis of bending in the beams was estimated from strain gauge readings taken at the tip of the slit damper (Fig. 21). As expected, the addition of the composite slab to the beam resulted in a neutral axis location for positive bending located nearer to the top of the sections than that of the bare

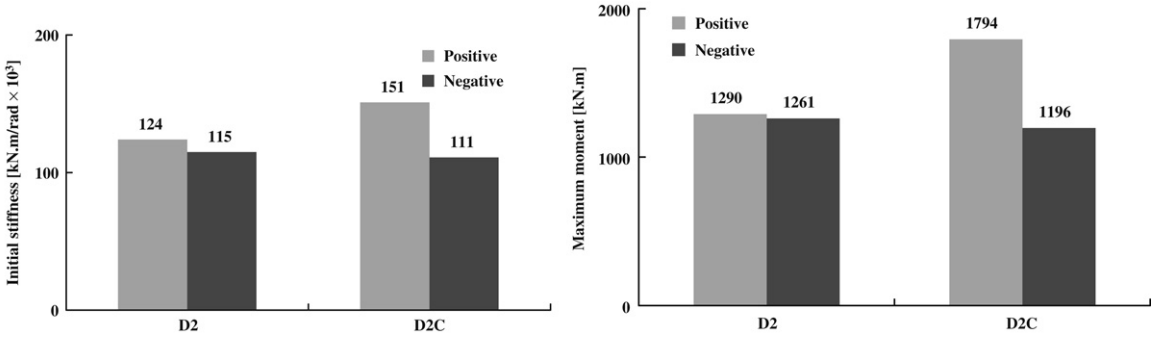

Fig. 20. Bar charts for the initial stiffness and the maximum moment.

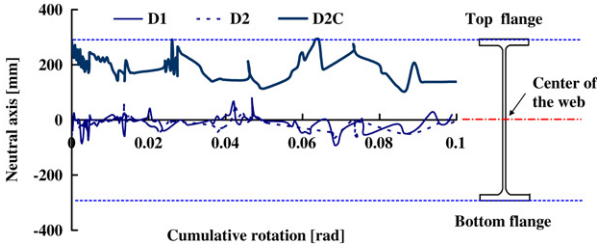

Fig. 21. Neutral axis for each specimen.

steel beams. Previous studies indicated that conventional welded moment connections fractured prematurely in a brittle manner at the bottom flange of the beam [33,34]. However, specimen D2C with a floor slab showed an excellent plastic deformation capacity. On the contrary, the skeleton rotation of D2 was significantly higher than that of D2C, as shown in Fig. 19. This was because the energy absorbed at the Bauschinger part was much greater than that at the skeleton part. This result demonstrates that, in designing the proposed connections, the effects of the composite beam should be considered.

5. Conclusions

In this study, a new structural system is proposed that features superior deformation capacity and ease of repair after an earthquake. The proposed connection is a beam-to-column connection system where the slit damper is connected to the bottom flange of the beam using high-strength bolts. To verify the performance of the proposed system, quasi-static cyclic tests were conducted on three full-scale specimens that had slit dampers and on one specimen that had a conventional welded connection. The key conclusions are noted below.

1. The proposed structural system exhibited stable hysteretic behavior under large story drift. The initial stiffness of the proposed connection can be viewed as a rigid connection, considering that the results are equal to or higher than the welded test specimen.
2. The proposed structural systems were designed so that the plastic moment of the beam section was not smaller than the maximum beam moment. Consequently, the plastic deformation was concentrated at the slit dampers while the beams and columns remained almost elastic.
3. The presented theoretical solutions of the initial stiffness and the yield strength based on the trilinear model of the slit damper of the proposed connections concurred well with both the test results and the FEA results and can be used effectively in predicting elasto-plastic behavior.
4. Compared with the steel connection, the initial stiffness and the maximum strength of the composite connection with slabs increased significantly. Test results showed that the plastic deformation capacities of specimens D2 and D2C were equal, while the skeleton rotation of D2 was significantly higher than that of D2C. This was because, for D2C, the energy absorbed at the Bauschinger part was much greater than that at the skeleton part. This result demonstrates that, in designing the proposed connections, the effects of the composite beam should be considered, even though the two specimens developed nearly the same plastic rotation.
5. The conventional welded specimen *W* also showed stable hysterectic loop and good plastic deformation capacity. However, the entire plastic deformation originated from the local buckling of the beam. Therefore, it is ineffective to repair these conventional welded connections after an earthquake.
6. It is believed that the energy absorption is concentrated only at the slit dampers rather than at the beams. Thus, the slit dampers can be replaced after an earthquake more readily than can beams and columns.
7. Unlike the bracing system, the load-carrying mechanism of the proposed structural system is not governed by shear force but by bending moment. This mechanism demonstrates that the proposed system is well suited for tall buildings where moment resisting structures are more efficient than brace frames. Further research is thus necessary to investigate the behavior of a structural system equipped with slit damper so that a more generalized evaluation of seismic capacity of the proposed system can be achieved.

References

[1] Miller DK. Lessons learned from the Northridge earthquake. Eng Struct 1998; 20(4–6):249–60.
[2] Nakashima M, Inoue K, Tada M. Classification of damage to steel buildings observed in the 1995 Hyogoken–Nanbu earthquake. Eng Struct 1998;20(4–6): 271–81.
[3] Tremblay R, Timler P, Bruneu M, Filiatrault A. Performance of steel structures during the 1994 Northridge earthquake. Canad J Civil Eng 1995;22(2):338–60.
[4] Architectural Institute of Japan. Reconnaissance report on damage to steel building structures observed from the 1995 Hyogoken Nanbu Earthquake. Kinki Branch (Osaka). 1995.
[5] Engelhardt MD, Winneberger T, Zekany AJ, Potyraj TJ. Experimental investigation of dogbone moment connections. AISC Eng J 1998;(4th quarter):128–39.
[6] Suita K, Tamura T, Morita S, Nakashima M, Engelhardt MD. Plastic rotation capacity of steel beam-to-column connections using a reduced beam section and no weld access hole design. AIJ J Struct Constr Eng 1999;526(12):177–84.
[7] Oh SH, Kim YJ, Moon TS. Cyclic performance of existing moment connections in steel retrofitted with a reduced beam section and bottom flange reinforcements. Canad J Civil Eng 2007;34(2):199–209.
[8] Federal Emergency Management Agency (FEMA). Recommended seismic design criteria for new steel moment-frame buildings. FEMA350. Washington (DC). 2000.
[9] Engelhardt MD, Sabol TA. Reinforcing of steel moment connections with cover plates: Benefits and limitations. Eng Struct 1998;20(4–6):510–20.
[10] Uang CM, Bondad D. Cyclic performance of haunch repaired steel moment connections: Experimental testing and analytical modeling. Eng Struct 1998; 20(4–6):552–61.

[11] Kim YJ, Oh SH, Moon TS. Seismic behavior and retrofit of steel moment connections considering slab effects. Eng Struct 2004;26(13):1993–2005.
[12] Kim YJ, Oh SH. Effect of the moment transfer efficiency of a beam web on deformation capacity at box column-to-beam connections 2007; 63(1): 24–36.
[13] Architectural Institute of Japan. Japanese architectural standard specification: JASS 6 steel work. Tokyo. 1996 [in Japanese].
[14] Nakashima M, Suita K, Morisako K, Maruoka Y. Tests of welded beam-column subassemblies. I: Global behavior. J Struct Eng 1998;124(11):1236–44.
[15] Suita K, Nakashima M, Morisako K. Tests of welded beam-column subassemblies. II: Detailed behavior. J Struct Eng 1998;124(11):1245–52.
[16] Wada A, Connor JJ, Kawai H, Iwata M. Damage tolerant structure. In: 5th U.S.-Japan workshop on the improvement of building structural design and construction practice. 1992. p. 1–12.
[17] Wada A, Huang YH, Iwata M. Passive damping technology for building in Japan. Prog Struct Eng Mater 2000;2(3):335–50.
[18] Symans MD, Charney FA, Whittaker AS, Constantinou MC, Kircher CA, John MW, Mcnamare RJ. Energy dissipation systems for seismic applications: Current practice and recent developments. J Struct Eng 2008;134(1):3–21.
[19] Tsai K, Chen H, Hong C. Design of steel triangular plate energy absorbers for seismic-resistant construction. Earthq Spectra 1993;9(3):505–28.
[20] Kobori T, Mirura Y, Fukusawa E, Yamada T, Arita T, Takenaka Y. et al. Development and application of hysteresis steel dampers. In: Proceedings of 11th world conference on earthquake engineering. 1992. p. 2341–6.
[21] Iwata M, Kato T, Wada A. Performance evaluation of buckling-restrained braces in damage-controlled structures. In: Behavior of steel structures in seismic areas: STESSA 2003. 2003. p. 37–43.
[22] Sabelli R, Mahin S, Chang C. Seismic demands on steel braced frame buildings with buckling-restrained braces. Eng Struct 2003;25(5):655–66.
[23] Iwata M, Murai M. Buckling-restrained brace using steel mortar planks; performance evaluation as a hysteretic damper. Earthq Eng Struct Dyn 2006; 35(14):1807–26.
[24] Tremblay R, Bolduc P, Neville R, Devall R. Seismic testing and performance of buckling-restrained bracing systems. Canad J Civil Eng 2006;33(2):183–98.
[25] Benavent Climent A, Oh SH, Akiyama H. Ultimate energy absorption capacity of slit-type steel plates subjected to shear deformations. J Struct Constr Eng 1998;503(1):139–45.
[26] Lee MH, Oh SH, Huh C, Oh YS, Yoon MH, Moon TS. Ultimate energy absorption capacity of steel plate slit dampers subjected to shear force. Steel Struct 2002; 2(2):71–9.
[27] Benavent Climent A. Influence of hysteretic dampers on the seismic response of reinforced concrete wide beam-column connections. Eng Struct 2006;28(4): 580–92.
[28] Chan RWK, Albermani F. Experimental study of steel slit damper for passive energy dissipation. Eng Struct 2008;30(4):1058–66.
[29] Koetake Y, Chusilp P, Zhang Z, Masakazu A, Suita K, Inoue K, Uno N. Mechanical property of beam-to-column moment connection with hysteretic dampers for column weak axis. Eng Struct 2005;27(1):109–17.
[30] Oh SH, Kim YJ. Hysteretic behavior of beam-to-column connections with slit plate dampers. J Archit Inst Korea Struct Constr 2005;21(12):101–8.
[31] Oh SH, Kim YJ, Ryu HS, Kang CH. Hysteretic characteristics of beam-to-column connections with energy absorption elements at beam bottom flanges. J Archit Inst Korea Struct Constr 2006;22(8):101–8.
[32] Inoue K, Suita K, Takeuchi I, Chusilp P, Nakashima M, Zhou F. Seismic-resistant weld-free steel frame buildings with mechanical joints and hysteretic dampers. J Struct Eng 2006;132(6):864–72.
[33] Kim YJ, Oh SH, Moon TS. Seismic behavior and retrofit of steel moment connections considering slab effects. Eng Struct 2004;26(13):1993–2005.
[34] Okada K, Oh SH, Yamada S, Imaeda T, Yamaguchi M, Wada A. Experimental study on deformation capacity of composite beams with conventional-type beam-to-column connections. J Struct Constr Eng 2001;547(9):161–8.
[35] Jones SL, Fry GT, Engelhardt MD. Experimental evaluation of cyclically loaded reduced beam section moment connections. J Struct Eng 2002;128(4):441–51.
[36] Korea Institute of Construction and Transportation Technology Evaluation and Planning (KICTTEP). Development of long, reusable, and recycling steel structural system. KICTTEP 04R & D A03-03. 2006.